

Visualization and interpretation of Rydberg states

Ladislav Kocbach[†] and Abdul Waheed^{†¶}

[†]Department of Physics and Technology, University of Bergen, N-5007 Bergen, Norway

[¶] Higher Education Commission of Pakistan, Islamabad, Pakistan

E-mail: ladislav.kocbach@ift.uib.no, waheed.tanoli@gmail.com

Abstract. For many purposes it is desirable to have an easily understandable and accurate picture of the atomic states. This is especially true for the highly excited states which exhibit features not present in the well known states hydrogen-like orbitals with usual values of the quantum numbers. It could be expected that such visualizations are readily available. Unfortunately, that is not the case. We illustrate the problems by showing several less fortunate earlier presentations in some scientifically most valuable works, and show more suitable visualizations for those cases. The selected cases are not chosen to criticize the authors' approach. Rather, we have taken these very important papers to underline the need for serious work with graphical representations which this work attempts to be a part of.

In this text we discuss the problems encountered when visualizing Rydberg states, review some existing presentations and propose guidelines for applications. The focus of this work are so called Stark states and coherent elliptic states of Rydberg atoms. In the sections on elliptic states we show some quite novel geometric interpretations which should be very helpful in analysis of Rydberg state manipulations in external fields.

Our demonstration examples involve only hydrogen-like states. However, the techniques and analysis are also relevant for Rydberg molecules and more complicated highly excited atomic and molecular systems.

1. Introduction

In theoretical physics it is sometimes assumed that once we have an analytical formula for a certain quantity, the problem is solved, this quantity is known and for many purposes in principle understood. For Rydberg states (see e.g. Gallagher [1]), whose analytic formulae are known since the first days of quantum mechanics this definitely is not the case. Even though their formulae are well known, the structures can show so much complexity of features that good visualization work is required. Ever since the first papers on the subject some graphical representations have been included both in textbooks and in scientific papers.

The wavefunctions for Rydberg states are after all hydrogen-like wavefunctions and the representation of hydrogen-like wavefunction appears in some form in many textbooks. They are also attractive for many popular science presentations. Recent offerings even include pictures similar to those discussed here. It might thus seem unnecessary to devote a special publication to such well known representations, but as we shall show, general type of visualization of such states offers several challenges and we will also discuss several previously published less fortunate cases. The main source of problems is that the application to large principal quantum number, i.e. weakly bound - or highly excited - states with many nodes, must show structures with many details which might appear at varying scales. For large quantum number n even the s-states, present some challenge.

In this paper we discuss generally the visualization of Rydberg states, with main focus on the so called Stark states and coherent elliptic states (CES), as well as some related high n states. In section 2 we discuss the seemingly straightforward visualization of probability densities or wave functions of the isotropic s -states and demonstrate the challenges present for highly excited Rydberg states and show possible solutions.

In section 3 we show the problems of Stark state visualization. They have axial rotational symmetry, thus in principle two dimensional cuts by a plane can be used, but it is demonstrated that a three-dimensional representation might be useful. In section 4 we list and shortly discuss the first set of unfortunate representations in scientifically important works.

The coherent elliptic states are presented in section 5. These states are truly three-dimensional and we discuss the method of visualization using isosurfaces and their modifications, with cuts and transparency properties. In this context a new type of visualization is discussed, but it is also shown that similar ones have been employed to related problems nearly 20 years ago.

Certain aspects of interpretation of coherent elliptic states are discussed in section 6. Here we again find some less fortunate visualization effects which propagate into future works. A classical picture is offered as an alternative intuitive justification, as well as a study of probability current density of the CES.

In the following section 7 we discussed new applications to a more general type of coherent superposed states and possible new insights in a contemporary project on

experimental studies of Rydberg atoms using electric and magnetic fields manipulations.

The visualization work reported in this paper is based on the package MATLAB by MathWorks. MATLAB is widely used in teaching mathematics and physics and in many areas of research. Similar techniques are however available in many different frameworks, some of them as free software. Thus the general features of the visualizations presented are certainly not limited to MATLAB.

2. Visualizing s-states

The s-states are radial functions only, thus a representation in terms of a single-variable plots should be sufficient to record the structure of the atomic state. There is still one step from knowing the radial dependence to visualizing how the spherical object really appears, but for most people this mental step is rather easy. One can imagine for example a cut through the sphere and on the cut to have displayed the map of the density. Every physicist has seen through the education such representations of Earth or other nearly spherical objects.

Plotting a function of one variable should not present any problem - but for hydrogenic states $\psi_{nlm}(\mathbf{r})$ with large values of n there appears immediately one problem - widely varying scale of magnitude from the smallest radial distances outwards. In figure 1 we illustrate the origin of this problem, here on the example of the radial function of an s-state $n=10$, $l=0$, a relatively low n .

The figure first shows a plot of radial wavefunction in section (a). Clearly the plot is not very useful for displaying the large r behavior on the scale of values relevant for small r . One straightforward method is simply to change scale, which naturally eliminates a good representation of the small r region, but that does not matter since one knows that the states contain the exponential decay modified by a combination of polynomials and thus is simply a monotonous steep fall with r until it enters the picture. It should however be kept in mind that there is a small radial region where the wavefunction peaks enormously for large n . Generally, Rydberg states have interesting structures and also majority of their probability density in regions where the actual probability density is low. Maximal values of the density appear close to the nucleus, but the total relative contribution of this is close to negligible.

Plot (c) is the well known type of plot often used in textbooks showing the radial probability density. The success of this plot is a root of problems and misunderstandings discussed below. It is so popular that sometimes "plot of radial density" is understood as this type of plot. One can misplace "radial dependence of density" - a well defined term with "radial density" - a term which does not have a unique definition, but is often understood as the shown picture (c). Textbook definition might be: *The radial probability density for the hydrogen ground state is obtained by multiplying the square of the wavefunction by a spherical shell volume element.* We see that this picture completely distorts the relative importances. The maximum values are unfortunately eliminated, so this representation conceals the fact of extremely high relative densities

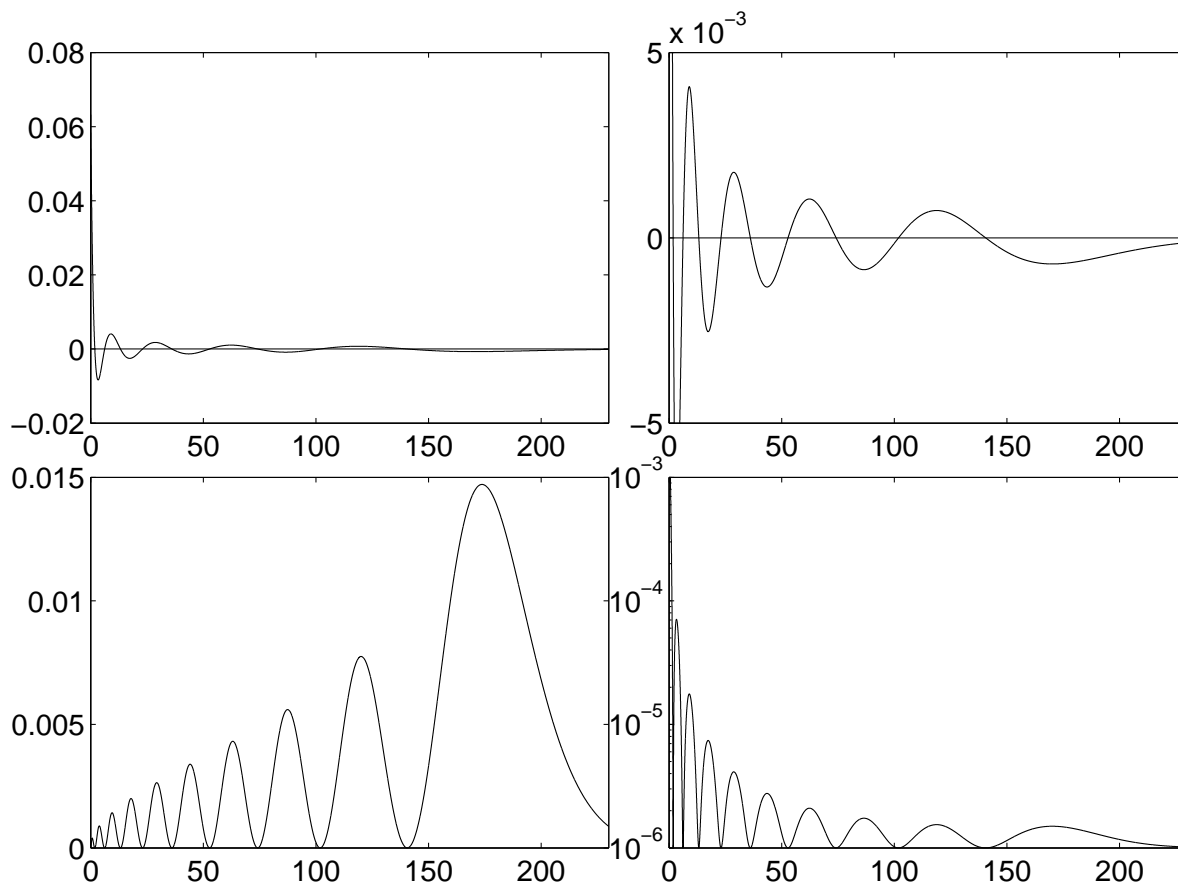


Figure 1. Plotting of radial wavefunctions and densities. Plot (a) shows the radial wavefunction plot for $n=10$, $l=0$. The plot is not useful, large r behavior is not represented. Plot (b) is the same with changed scale, which naturally eliminates a good representation of the small r region. Plot (c) is the well known plot showing the radial probability density. The success of this plot is a root of the discussed problems. Plot (d) shows a starting point for the discussed solution: real probability density is plotted, but in the form of its logarithm, with cut-off for small values (large negative logarithm cut-off). This last plot illustrates that the logarithmic plotting might make it possible to construct good representations of the wavefunction (probability) structures for Rydberg states.

at the nucleus and exaggerates the values at large distances.

Plot (d) shows a starting point for one of our proposed solution: actual probability density is plotted, but in the form of its logarithm, with cut-off for small values (large negative logarithm cut-off). This last plot illustrates that the logarithmic plotting might make it possible to construct good representations of the wavefunction (probability) structures for Rydberg states. It is a well known technique to show multi-scale dependencies.

The problems discussed here for states with maximum symmetry become necessarily much more complex for states with less symmetry and the visualization task becomes much more difficult. In the next section we shall show how this has been a cause of

more or less confusing information in the literature.

When moving to general n , l , m , the densities of states for all of these are rotationally symmetric with respect to z-axis, since they are eigenstates of L_z . Thus for any n , l , m , state a plot in terms of 2 variables is sufficient for all n , l , m , states.

$n00$	simple radial plot
nlm	plot of a plane cut (x, z) - 2 variable plot
superposition	depends on x, y, z, 3-dimensional

It is thus clear that for a unified presentation, we need some methods to present the $|\Psi(x, y, z)|^2$

3. Stark states

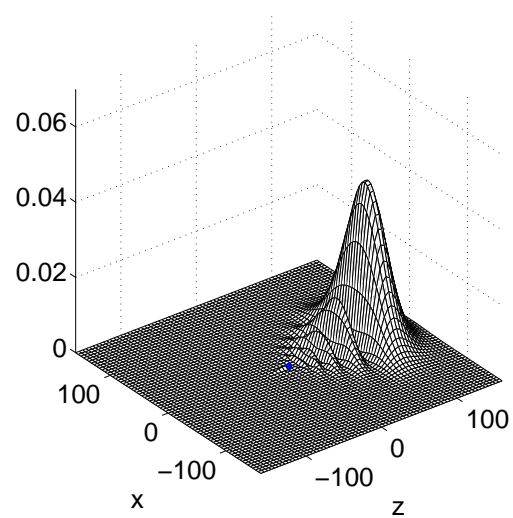
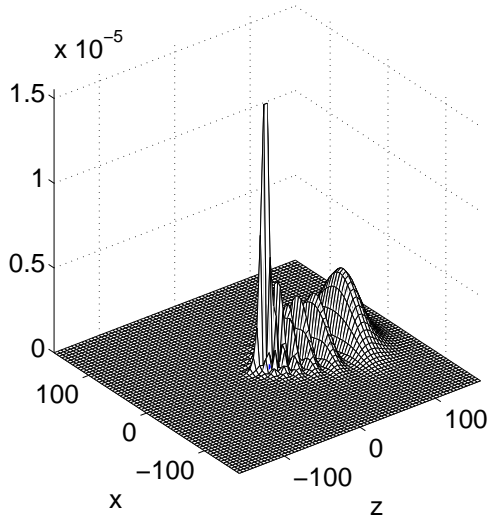
Already in his 1926 paper Pauli ([2], note the English translation available) described the solutions of Schrödinger equation for electrons in electric and magnetic field, and he has built on already published earlier works, so some of the aspects discussed here have been part of the general knowledge from the beginning of the Quantum mechanics. The states in electric field only, without magnetic field, are important for understanding of the Stark effect and it has become usual to refer to these states as Stark states. Instead of the quantum numbers n , l and m the Stark states are characterized by quantum numbers n , k and m , i.e. the angular momentum quantum number l is replaced by the Stark quantum number k . Sometimes one is using the parabolic quantum numbers n_1 and n_2 (e.g. Gallagher's book [1]), but the notation with quantum number k mentioned above is more symmetric and will be of particular advantage in section 7 on crossed electric and magnetic fields.

While the usual spherical states are eigenstates of L^2 the Stark states are eigenstates of the coordinate z , or in some sense more precisely the Runge-Lenz operator. For the purpose of the present discussion we limit ourselves only to the summary of Stark state properties.

With this usual definition the Stark states have cylindrical symmetry with z-axis as the symmetry axis. This property they share with the usual set of spherical eigenstates which are also characterized by the magnetic quantum number m . With cylindrical symmetry the probability densities are functions of two variables. As in the s-states case discussed in section 2 their display can be accomplished in a lower-dimensional space, in this case as a function of two variables. The problems will be very similar in this case, but amplified by the broader variation of possible display methods.

Probably the oldest way to display function of two variables are the maps showing the heights using equal height curves (contour maps) or color coded representations. They are most precise and suitable for displaying shapes of the different areas, since they are seen "from above" and preserve the x-axis and y-axis (in this case the cylindrical ρ and z along the electric field direction). Another possibility which became very popular in the first powerful years of computer graphics (say the 1980's) is a quasi-

Probability density Stark State r^0 $n=8, k=-7, m=0$ Probability density Stark State r^2 $n=8, k=-7, m=0$



Probability density Stark State r^0 $n=8, k=-7, m=0$

Probability density Stark State r^2 $n=8, k=-7, m=0$

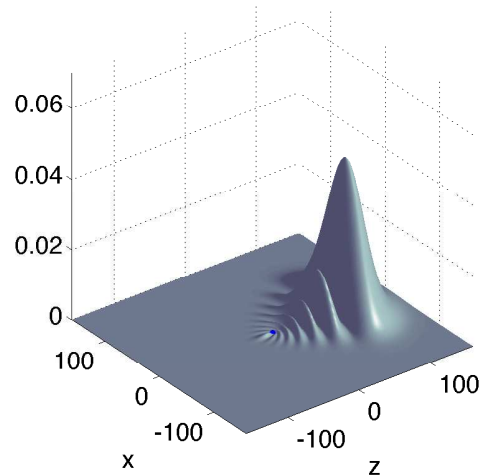
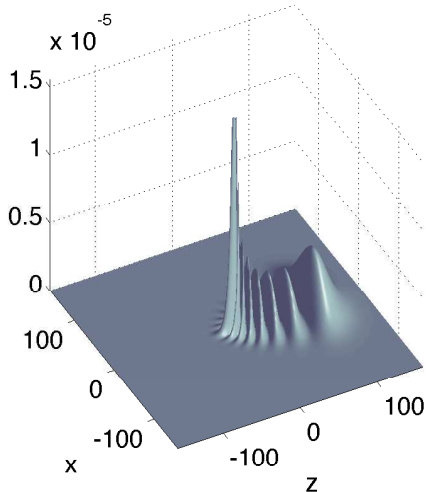


Figure 2. Landscape pictures of Stark states. The top row is using a type of appearance usual in the 1980's. (a) is constructed in similar way as in the s-states case: a cut-off is introduced. (b) The same data modified to avoid the nuclear peak problem - multiplied by r^2 . In the second row, the same plots with a more modern appearance, the polygons are replaced by continuous shading.

three-dimensional plot where one generates the landscape plot of the function of two variables.

One would usually choose not to plot only the defined positive ρ , but would rather show a cut through the density function e.g. along the (x-z)-plane, showing an reflection symmetric pattern of the density.

The landscape plots examples are shown in figure landscape-stark. If we start plotting the $|\Psi(x, y, z)|^2$ we quickly encounter the same problem of the very high nuclear maximum - and the same methods as discussed in section 2 apply here. But now

we can confuse the issues even more. We can choose to plot a sort of radial density $2\pi\rho|\Psi(x, y, z)|^2$ in analogy with the spherical definition. That might not help much, the nuclear peak in the landscape map still remains very prominent. Thus during the years many people have chosen to plot $r^2|\Psi(x, y, z)|^2$ also in this case.

This choice has the advantage to display all the regions, but it has many disadvantages. First of all, one must not forget to mention what is actually plotted. Many people through the years and even most recently forget to do that. Second, the shapes might be quite distorted relatively, it might be necessary to choose varying viewpoints for different functions and so on.

One unfortunate accident is that a display of these problems can be quite exactly illustrated by Figure 6.1 of the classic work, Gallagher's book *Rydberg Atoms* ([1], page 73). The figure appears to be a type of reprinted information so that the author can be not fully responsible for the missing and slightly misleading information (the caption says "Charge distribution for H for parabolic eigenstates", but what is plotted are the modified distributions, i.e. multiplied by a power of r , as far as we can see by the factor r^2). The main point of the figure caption is the illustration of the induced dipole moments - and that point is definitely correct.

To complement this excellent classic book by Gallagher we bring here our version of its figure 6.1 on page 73 in the present figure 3.

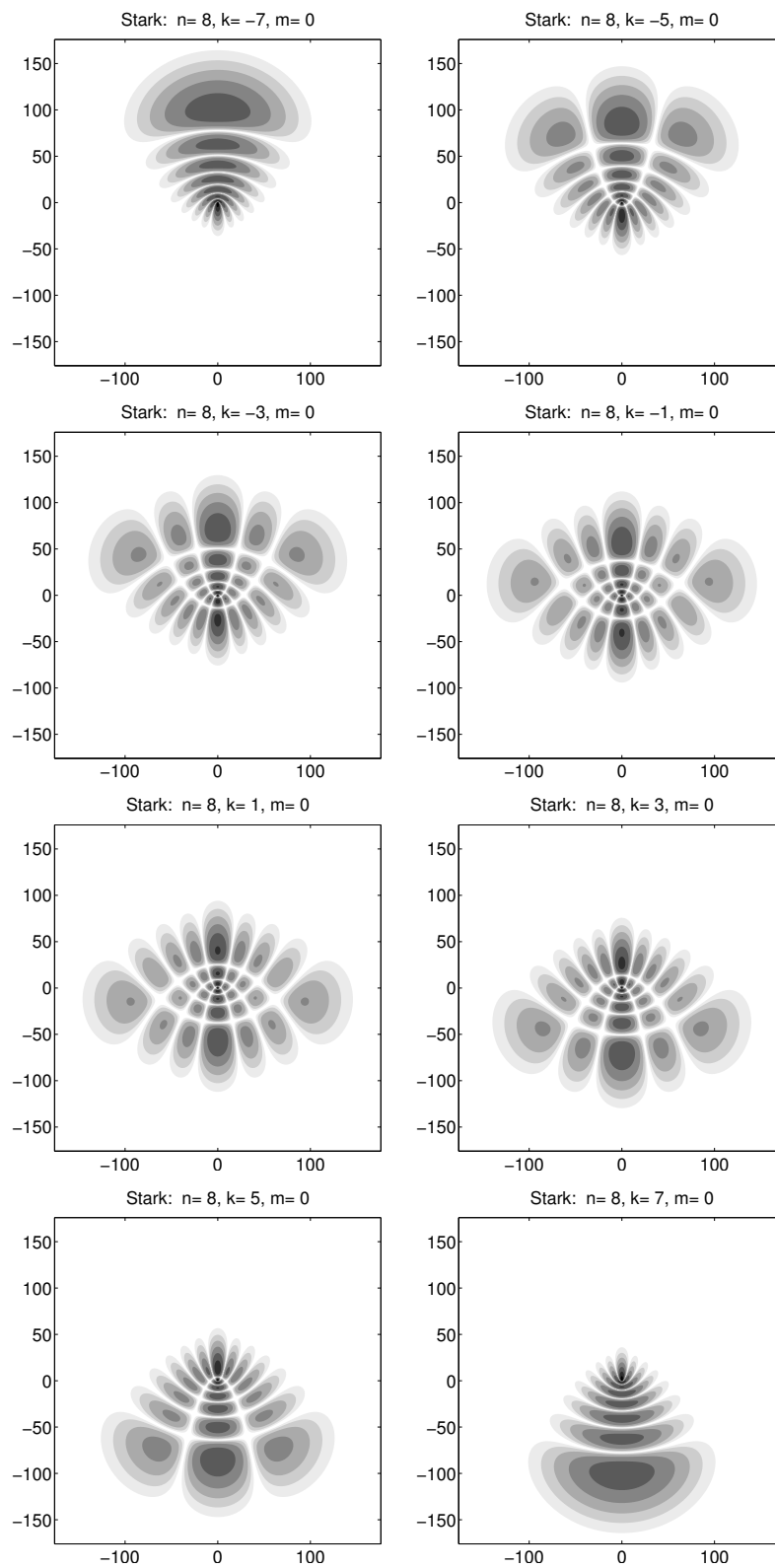


Figure 3. Replacement for Gallagher Rydberg atoms figure 6.1. This type of plot is to be preferred. The density is visualized by plotting a contour plot of the logarithm of the density, as used also in the one-dimensional case of radial density in figure 1

In order to make the content of figure 3, i.e. the maps of probability density (which use logarithmic representation, each new shade denotes an increase by about a factor

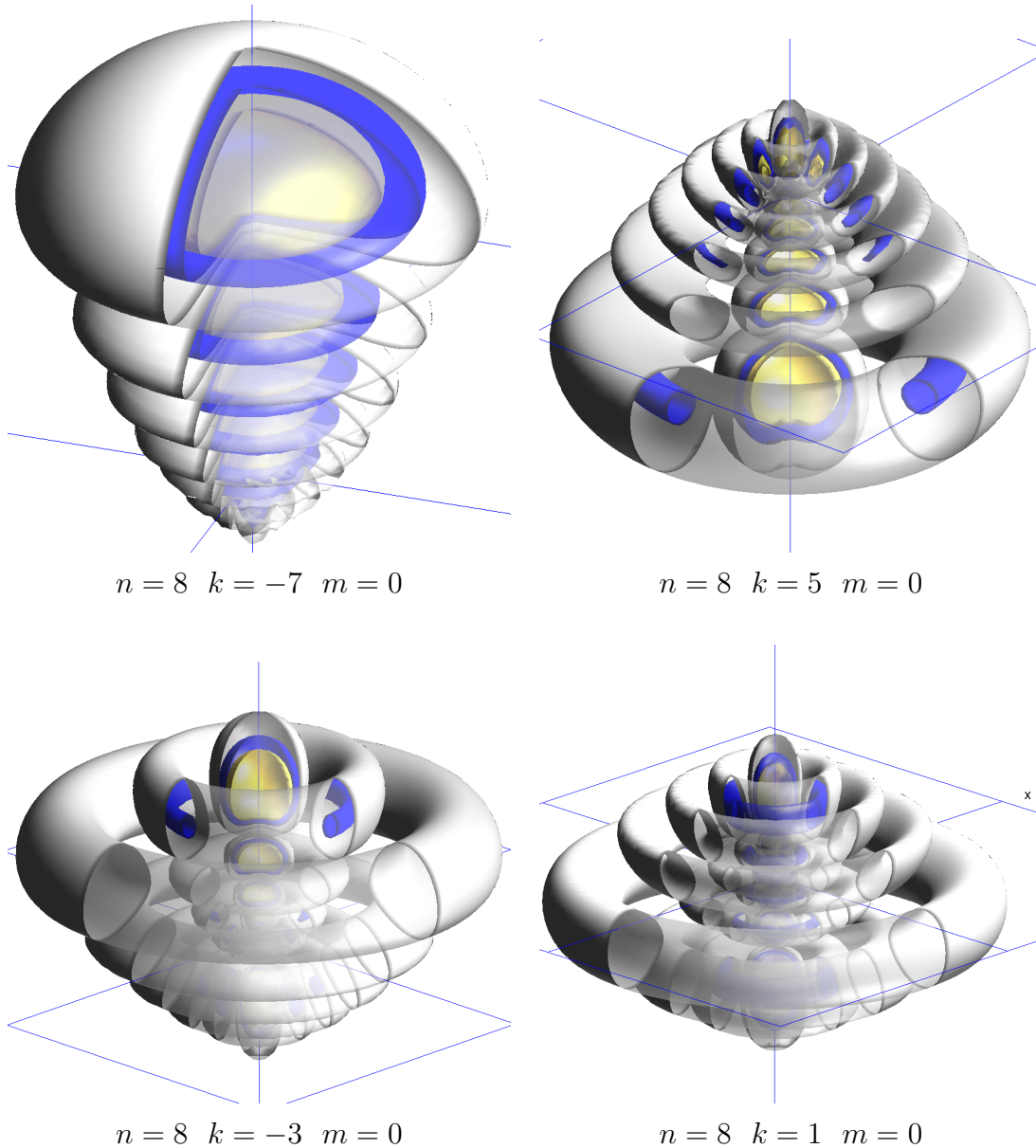


Figure 4. The figures $n = 8$, $|k| = 1$ to 7 , $m = 0$ are plotted. we take $k = -7$, $k = 5$, $k = -3$ and $k = 1$ to show the various features

e) more intuitive, we show a different three-dimensional representation of the shapes in figure 4. In this figure we repeat only the four differing shapes in the table of eight, alternating the positive and negative values from 7 to 1.

This type of figures will be discussed in more detail below, here we just mention that these are iso-surface plots, three-dimensional generalisation of the contour plots. To show the inner structure of the distributions, part of the isosurfaces are made transparent. Here only three values of density are used. The densities are normalized

n=5					
m	l				
-4	4				
-3	4	3			
-2	4	3	2		
-1	4	3	2	1	
0	4	3	2	1	0
1	4	3	2	1	
2	4	3	2		
3	4	3			
4	4				

n=5					
m	k				
-4				0	
-3			-1	1	
-2			-2	0	2
-1		-3	-1	1	3
0	-4		-2	0	2
1		-3	-1	1	3
2			-2	0	2
3			-1	1	
4				0	

Table 1. Stark states combinations of hydrogen atom for $n = 5$ to the right, compared to the states of spherical basis arranged in similar manner to the left

n=4				
m	l			
-3	3			
-2	3	2		
-1	3	2	1	
0	3	2	1	0
1	3	2	1	
2	3	2		
3	3			

n=4				
m	k			
-3			0	
-2			-1	1
-1		-2	0	2
0	-3		-1	1
1		-2	0	2
2			-1	1
3			0	

Table 2. Stark states combinations of hydrogen atom for $n=4$ to the right, compared to the states of spherical basis arranged in similar manner to the left

by factors of n^6 -type and isosurfaces with values 0.5, 2 and 4 are used. No logarithmic scale is used in this case.

Note that all the states shown in figures 3 and 4 are $m = 0$ states, it means they are unique and they are real functions, it means the numerous "tubes" do not enclose any currents. Usually such tubes appear for $|m| > 0$ states where they 'enclose' an "azimuthal" current, since for $|m| > 0$ the wavefunctions contain a factor $\exp(im\phi)$ as in the spherical harmonics. It should however also be mentioned that quite rich structures of somewhat similar type are also obtained for high n and l with $m=0$.

The $m = 0$ states are not the only possible states. For a given n , there are exactly n states with $m = 0$ while there are n^2 various Stark states. As an example, we compare the states of $n=5$ (table 1) and $n=4$ (table 2)in the two quantization schemes, the spherical system and the parabolic system.

We show both of the tables, since they demonstrate one interesting feature: only for odd values of n we can have the state $k = 0$ $m = 0$ which has both cylindrical symmetry ($m = 0$) and reflection symmetry along the z-axis ($k = 0$). For n even such

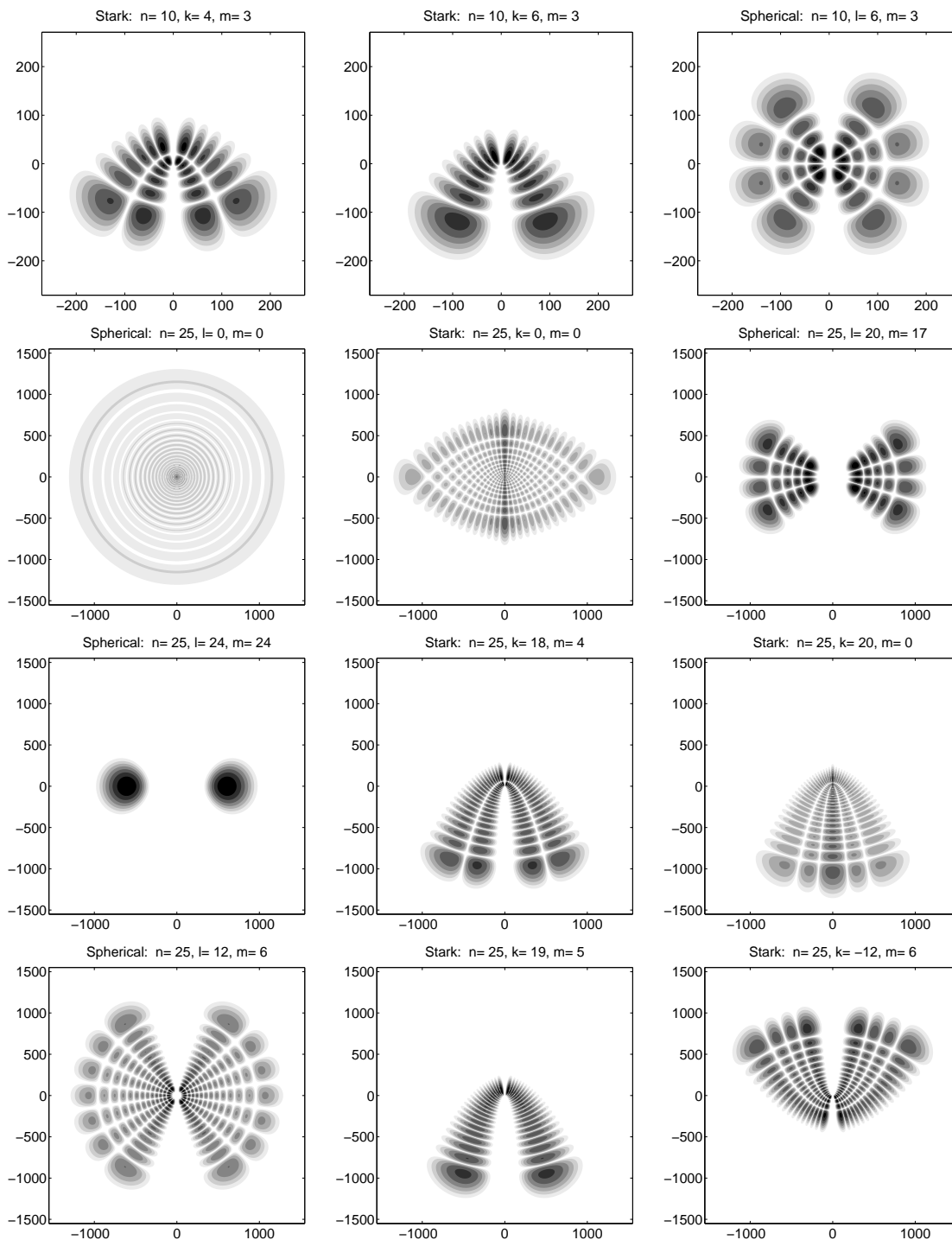


Figure 5. Example plots of Rydberg states. Note that all the states are cylindrically symmetric, i.e. the full shape is a rotation along the vertical z -axis. The states $m = 0$ will have a solid block along the z -axis, all the $m > 0$ states have an empty tube - or a sort of funnel along the z -axis. Note the tiny black spot on the nucleus in the $25s$ state. Note also that generally there are high density regions close to the nucleus in most cases.

state does not exist. The $k = 0$ $m = 0$ states for large values of n have a very striking and unexpected structure - they are also reflection symmetric, but they only exist for odd n .

4. Unfortunate representations of Stark states

The first example is the famous figure 6.1 of Gallaher book discussed above, where the density is multiplied apparently by a power of r . This even without mentioning this multiplication. Our figure 3 shows our opinion of how the figure should have been presented. It is interesting to analyze why the original author of the figure chose this extra multiplicative factor so strongly modifying the shapes (as shown in our figure landscape-stark). It is very probable that the main reason is simply the wish to eliminate the uncomfortable nuclear maximum. Note that the height of this maximum relative to the last radial maximum (for density) scales roughly with n^4 , while its volume is of the order of one atomic unit of volume independent of n . The multiplication then propagates and leads to confusions and omissions, originally caused by inadequate visualization approach.

The next unfortunate choice we refer to has been made by Greene et al [4] In this case the authors correctly describe what the plot really is, quoting their figure caption: "A cylindrical coordinate surface plot of the electronic probability density, $2\pi\rho|\psi(\rho, z, 0)|^2$ and $2\pi\rho|\psi(\rho, z, \pi)|^2$ ". The plot is a part of a physically very important and motivating paper. However, the chosen representation is rather unfortunate because the central region along the internuclear axis which in fact is a maximum appears as being a node. It is a node due to the multiplication by the cylindrical ρ . Also, the authors even write "trilobite resembling density" which further strengthens the impression of flatness, while the object has cylindrical symmetry.

This unfortunate choice of representation has been continued to a recent paper in Science by W. Li *et al* [5] where the same method is used, but unfortunately in this case again omitting to specify this. The text inside of the figure even explicitly indicates an erroneous $|\Psi(r, R_0)|^2$, not including the ρ , which however is indicated as an axis denotation. This is clearly only an omission, but again the choice of the visualization method is unfortunate. In this case even more so, since the main character of the state is $35s$.

Similar example of unfotunate choice of interpretation for the next type of states will be discussed in section 6.

5. Coherent Elliptic States and other Coherent superpositions

5.1. Pauli's treatment of hydrogen atom in electric and magnetic fields

In 1926 Wolfgang Pauli presented the problem of a hydrogen atom in external fields [2]. Here he showed that (originally in the matrix formulation of quantum mechanics) how the stationary states of the hydrogen atom can be treated in classified using a

combination of angular momentum operator and the operator known today as Laplace-Runge-Lenz operator. The Hamiltonian for atomic hydrogen in a combination of electric (\mathbf{E}) and magnetic (\mathbf{B}) fields is given by

$$H = H_0 + \mathbf{E} \cdot \mathbf{r} + \frac{1}{2} \mathbf{B} \cdot \mathbf{L}, \quad (1)$$

with

$$H_0 = -\frac{\nabla^2}{2} - \frac{1}{r}, \quad (2)$$

being the Hamiltonian of an unperturbed hydrogenic atom, and the angular momentum operators of the electron is given by $\mathbf{L} = \mathbf{r} \times \mathbf{p}$.

When the dynamics is restricted to a single hydrogenic n -shell the Pauli's operator replacement can be

$$\mathbf{r} = \frac{3}{2} n \mathbf{A}, \quad (3)$$

where \mathbf{A} is the quantum mechanical counterpart of the classical Runge-Lenz vector,

$$\mathbf{A} = \frac{1}{\sqrt{-2H_0}} \left[\frac{1}{2} (\mathbf{p} \times \mathbf{L} - \mathbf{L} \times \mathbf{p}) - \frac{n}{r} \mathbf{r} \right]. \quad (4)$$

Pauli recognized that one can combine the operators \mathbf{L} and \mathbf{A}

$$\begin{aligned} \mathbf{J}_1 &= \frac{1}{2} (\mathbf{L} + \mathbf{A}), \\ \mathbf{J}_2 &= \frac{1}{2} (\mathbf{L} - \mathbf{A}), \end{aligned} \quad (5)$$

to two basically independent operators which obey the commutation relations of angular momentum, and can be used as independent operators. However, already Pauli have shown that these two operators are not fully independent. For states inside one n -shell their squares must have the same eigenvalue, $J_i^2 \rightarrow j_i(j_i + 1)$, $j_i = \frac{n-1}{2}$.

Then, the Hamiltonian of the intrashell system can be transformed using the pseudospins operators and the energy replacement, $H_0 = -1/2n^2$ it gets the form

$$H = H_0 + \boldsymbol{\Omega}_1 \cdot \mathbf{J}_1 + \boldsymbol{\Omega}_2 \cdot \mathbf{J}_2, \quad (6)$$

The vectors $\boldsymbol{\Omega}_1$ and $\boldsymbol{\Omega}_2$ are also given by a simple relation

$$\begin{aligned} \boldsymbol{\Omega}_1 &= \frac{1}{2} \mathbf{B} + \frac{3}{2} n \mathbf{E}, \\ \boldsymbol{\Omega}_2 &= \frac{1}{2} \mathbf{B} - \frac{3}{2} n \mathbf{E}, \end{aligned} \quad (7)$$

and resemble the role of two effective magnetic fields, since they appear in the same relation as \mathbf{B} and \mathbf{L} in equation (1).

In equation 7 the two operators \mathbf{J}_1 and \mathbf{J}_2 are defined as two vector operators, and from the definitions it follows that their components can be chosen with respect to any set of axes (6).

Diagonalization of the transformed hamiltonian eq. (6) is thus elementary. If we chose as basis states which at the same time are eigenstates of $J_{1z'}$ and $J_{2z''}$ where axis

z' is in the direction of $\mathbf{\Omega}_1$ and z'' the direction of $\mathbf{\Omega}_2$. We do not know these states $|m_1 m_2\rangle$ explicitly, but they are defined by the property

$$J_{1z'}|m_1 m_2\rangle = m_1|m_1 m_2\rangle \qquad J_{2z''}|m_1 m_2\rangle = m_2|m_1 m_2\rangle$$

Generally, for a given E and B these quantum numbers are not related in any way to the quantum numbers m or k discussed in section 3.

$$E_{m_1, m_2} = m_1 \Omega_1 + m_2 \Omega_2 \tag{8}$$

where Ω_1 and Ω_2 are the "lengths" of the two vectors in equation 7. When B and E are perpendicular, these two constants are equal and we obtain a set of states which have a structure similar to table 3 single state on the top and bottom with equidistant eigenvalues with increasing degeneracy by one from bottom towards the middle and again decreasing towards the top. The n^2 states plotted at positions of their eigenvalues form a diamond with middle width n and height n .

When E and B are not perpendicular the above equations are still valid but the eigenvalues do not show any particular symmetry and the degeneracy is mostly lifted.

5.2. Interpretations of CES

The two extreme states $|m_1 = -\frac{n-1}{2}, m_2 = -\frac{n-1}{2}\rangle$ and $|m_1 = \frac{n-1}{2}, m_2 = \frac{n-1}{2}\rangle$ have been called coherent states, from the point of view that they have minimum uncertainties of the involved operators. These coherent elliptic states (see e.g. Bommier et al [3]) are 3-dimensional objects, in the sense that their densities varies in all three dimensions with only one symmetry retained - the reflection symmetry. In order to visualize such states one then needs to represent a function of three variables in the two-dimensional geometry of the paper or screen - it means some three-dimensional help-objects must be used. There is a well established method of isosurfaces, i.e. plotting surfaces where the functional value remains the same. This is an extension of the contour plot used above to 3 dimensions. Often only one value is used, in our case a small value whose isosurface would enclose all the higher values of density.

This method we shall be using in the following, with some variations. Very useful method is to use several isosurfaces, using both transparency of the objects and cuts or slices. Technically, these methods are available in many packages, as already mentioned we use the package MATLAB. General feature of all such packages is that they should not be used with the standard parameters, adjustment of parameters is an essential part of the visualization work.

Plots recognizing this and somewhat resembling our type of plots (with 1990's graphics) have been presented for a somewhat similar problem of elliptic coherent states for two dimensional harmonic oscillator in [13]. The term coherent is also used in the same sense, when the quantum fluctuations are as small as possible considering the uncertainty relations for observables related to the orientation and the eccentricity e of an ellipse. These states are simple to construct and their wavefunction is localized on

the corresponding classical elliptical trajectory. With increasing principal quantum n , the localization on the classical invariant structures is more pronounced.

We start here by presenting our version of representation of Bommier's et al CES with the help of isosurfaces. Figure 7 shows a relatively strong electric field, but in fact one only leading to eccentricity, $e = 0.71$. Here the ellipse starts to get features of the Stark states apparent here as the extra rib. Figure 6 shows a typical CES for eccentricity $e = 0.55$.

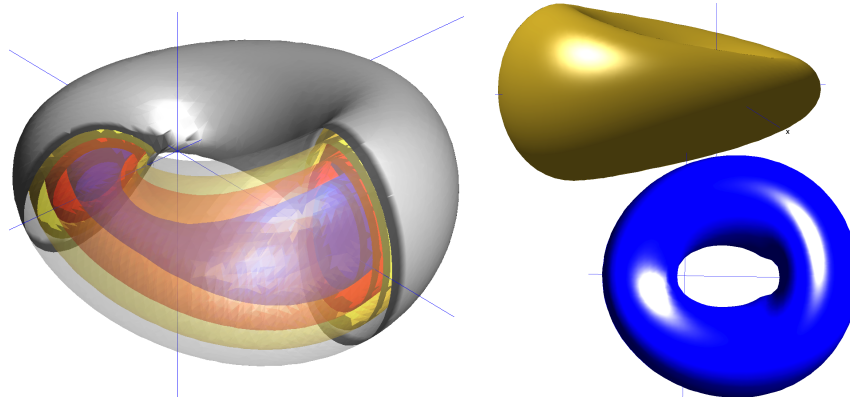


Figure 6. Elliptic state with $n=11$ and Bommier's $\alpha = 0.583$. Electric field is not too strong. The evaluated eccentricity is $e=0.55$.

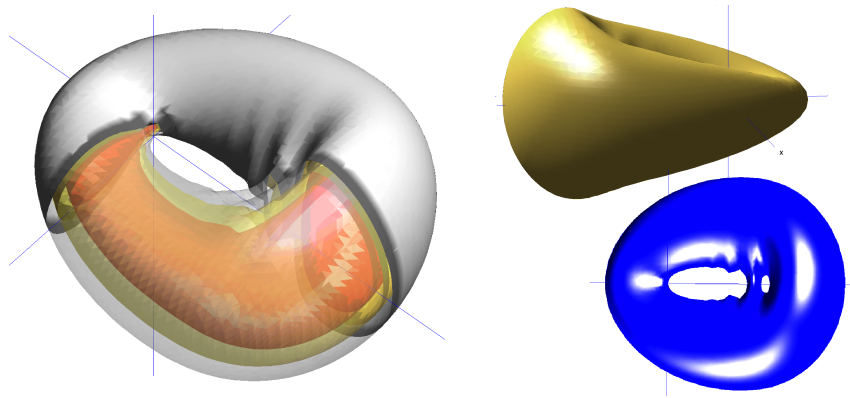


Figure 7. Elliptic state with $n=11$ and Bommier's $\alpha = 0.8$. Electric field is quite strong and the ellipse starts to get features of the Stark states (the extra rib). The evaluated eccentricity is $e=0.71$.

Probability density current is present in the circular states, i.e. in the states which are made possible by magnetic field. If we think about a possible preparation of such state, exposure to magnetic field defines its direction as a quantization axis and orders the states according to their magnetic quantum numbers, i.e. eigenstates of $\mathbf{L} \cdot \mathbf{B}$. The two circular states with maximum possible absolute value of $(n-1) B$ are also eigenstates of L^2 , while all the other states are not eigenstates of L^2 . They are degenerate and can be

chosen to be classified by L^2 as in the table 1. Similarly, the Stark states can be chosen by the electric field in the z -direction, and then they can be additionally characterized by the m_z quantum number, as shown in table 1.

However, only when the electric and magnetic actions are perpendicular one can obtain states which approach the elliptic states. Construction of all the n^2 states is straightforward by numerical diagonalization. Bommier et al have analyzed in great detail the analytic construction of the lowest state, which is coherent in the sense that it minimizes the variation in L_z and A_x . This aspect has been discussed already by Pauli, but not to the same depth. In perpendicular crossed fields, when B defines the z direction, the two extreme states change between circular (plus and minus orientation) in the x - y plane to linear Stark in positive and negative x -direction (E defines x -axis). Bommier et al derived an analytic expression for these states in terms of a summation over the (n, l, m) states.

In discussion of these states a serious misunderstanding has been propagated from the earlier discussed cases, i.e. that the densities must be transformed in order to avoid intuitively uncomfortable features.

6. Interpretations of Coherent Elliptic States

The coherent elliptic states have been discussed by Bommier et al, in several papers. In

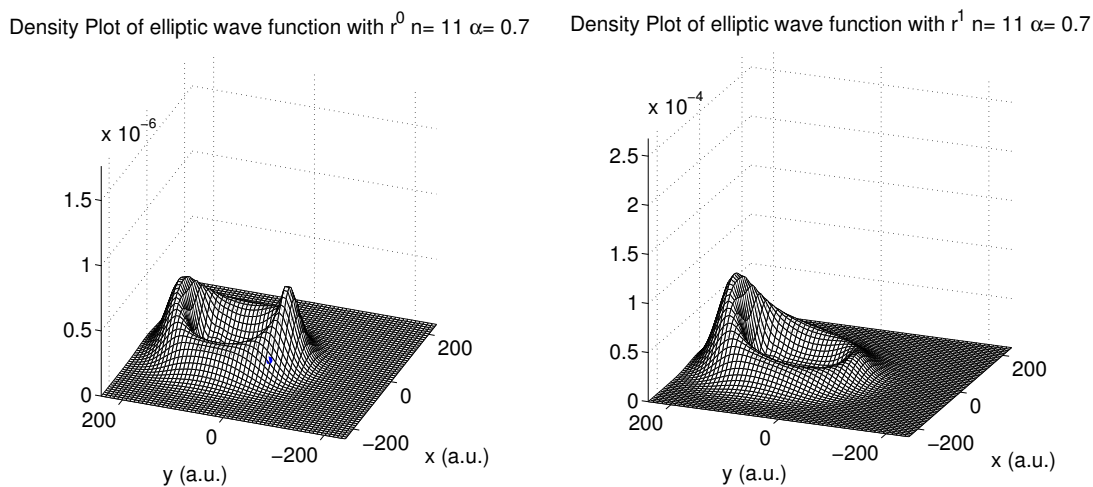


Figure 8. Elliptic state with $n=11$ and Bommier's $\alpha = 0.7$. The actual density shown to the left has maximum both at aphelion and at perihelion. The right picture shows one possible transformation attempting to avoid the peak at perihelion.

1989 J.-C. Gay, D. Delande and A. Bommier [14] introduce the *Atomic quantum states with maximum localization on classical elliptical orbits* On their figure 1(a) they show a plot of the electronic density in the (x, y) plane, showing localization on the ellipse. In Figure 1(b) they show a very a very illustrative cut in the perpendicular (z, x) plane showing that the elliptic state is strongly localized near the $z = 0$ plane, a very nice

feature to some degree showing the wedge shape of the elliptic states.

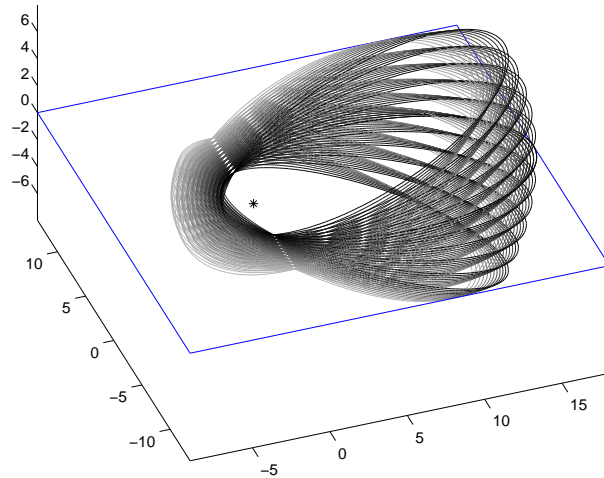


Figure 9. Classical elliptic trajectories with angular momentum uncertainty. This illustration displays increased density at the perihelion.

Then they add a completely unnecessary figure 1(c), (equivalent to the right part of our figure 8 which they describe as “... represents the electronic density in the (x, y) plane after averaging over z motion. It is still localized on the ellipse and the distribution is peaked at aphelion (minimum velocity) as expected from semiclassical arguments. The peaking at the perihelion (maximum velocity) which Fig. 1(a) exhibits is smoothed out”.

The smoothing is once more mentioned also in the figure caption, there as “The maximum at perihelion has been smoothed out. The one at aphelion is expected from semiclassical arguments.”

There is absolutely no need to smooth out the maximum at the perihelion. This maximum is present in all the elliptic trajectories, even for the states discussed in section 7. The authors did not like this maximum and tried to get rid of it by modifying the results.

Many scientists have since then been influenced by this misunderstood necessity of smoothing out the unwanted maximum. We refer here to one more example of an important review co-authored by one of our close collaborators, the review of *Charge transfer from coherent elliptic states* [15]. In their figure 4 the authors show the “smoothed” density introducing it as *The probability distribution projected onto the plane of the orbital is concentrated near a classical elliptic path.*, i.e. now the smoothing is described as a *projection*. Further the caption of the figure states that *The electron is more likely to be found at aphelion far from the nucleus, at the left side along E , than at perihelion close to the nucleus, at the right side.*

The last statement is true, but can not really be seen from the figure. It seems that it is in fact an attempt to formulate in physically correct terms the original smoothing argument for removing the perihelion density maximum.

The figure has no other role in this important review paper than an illustration, but it is a pity that this illustration repeatedly propagates an unfortunate misunderstanding. In our figure 9 we sketch one possible illustration of the perihelion maximum. All the classical elliptic trajectories corresponding to elliptic paths displaying the uncertainty in the angular momentum - and thus present in other (tilted)planes than the x-y plane, must pass through a rather narrow region close to the perihelion of the ellipse in the x-y plane. This can lead to a maximum, even if the higher velocity for each individual orbit would lead to a minimum.

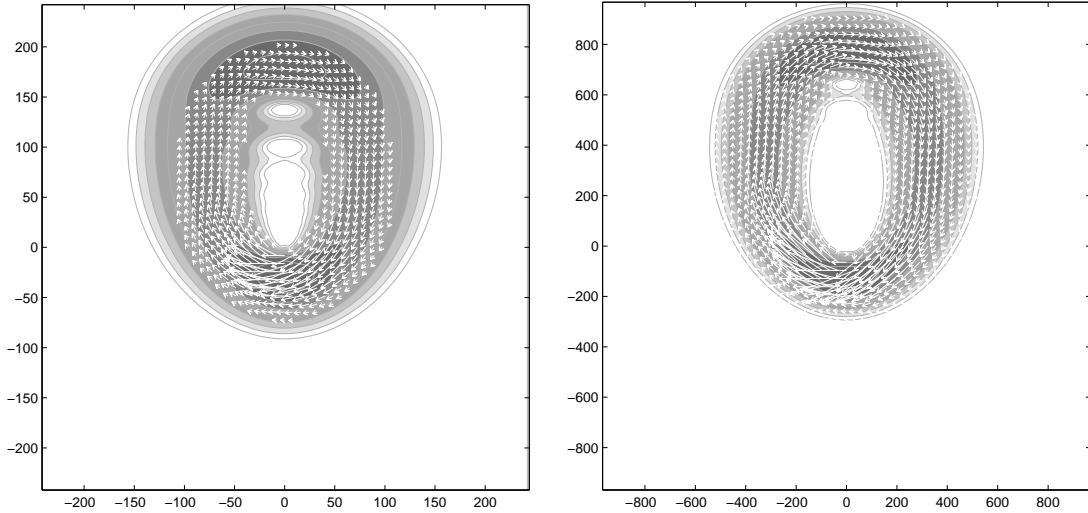


Figure 10. Elliptic states for $n = 11$ and $n = 22$. Plotted is probability density in the x-y plane as for the plots in figure. The white arrows show the probability density current. The arrows are shown only for values larger than interactively set threshold. The length of the arrows is in a nonlinear way proportional to the current density. The plotting method has been developed in our studies [18] of atomic collisions in the 1990's.

This argument, however might not be too precise. To provide indication of what else could be done with the interpretation of these coherent states we have added simple diagrams of probability density ρ and probability density current \mathbf{j}

$$\rho(\mathbf{r}, t) = \psi^*(\mathbf{r}, t)\psi(\mathbf{r}, t) \quad \mathbf{j}(\mathbf{r}, t) = \frac{1}{2i}[\psi^*(\mathbf{r}, t)\nabla\psi(\mathbf{r}, t) - \psi(\mathbf{r}, t)\nabla\psi^*(\mathbf{r}, t)](9)$$

7. Rydberg States in Crossed Electric and Magnetic Fields

In experimental work the Rydberg atoms will often be manipulated by crossed perpendicular electric and magnetic fields. This problem has been also discussed by Pauli already in 1926 and most of the mathematical structure was identified by Pauli already then, as is summarized here in section 5.1.

For the discussion here we reconstruct the $n = 5$ (table 1) with a change as table 3. In the right hand side of table 3 we have interchanged the meaning of the quantum

numbers m and k , to adjust this to the situation when the axis defining k is x-axis and not z-axis.

n=5					
m_z	l				
-4	4				
-3	4	3			
-2	4	3	2		
-1	4	3	2	1	
0	4	3	2	1	0
1	4	3	2	1	
2	4	3	2		
3	4	3			
4	4				

n=5							
k_x	m_x						
-4					0		
-3				-1		1	
-2			-2		0		2
-1		-3		-1		1	3
0	-4		-2		0		2
1		-3		-1		1	3
2			-2		0		2
3				-1		1	
4					0		

Table 3. Stark states combinations of hydrogen atom for $n = 5$ to the right, compared to the states of spherical basis arranged in similar manner to the left

Here we shall show some surprising features of the transition from circular states to linear Stark states. The Coherent elliptic state behaviour is well known. In figure 11 the CES is shown to the left (blue in the color print version). The other two columns are the next two states which are degenerate in for all combinations of E and B as far as they remain orthogonal.

We can see that while the CES has one ring, transforming from the circular to the elliptic (flat structure close to the x-y plane), the two qCES have two rings, configured in very distinct ways (inside or above each other). We also see that the CES develops into a cylindrically symmetric ($m_x = 0$) shape, i.e. not flat, the two qCES are transformed to two flat objects, one close to the x-y plane, the other close to the perpendicular x-z plane.

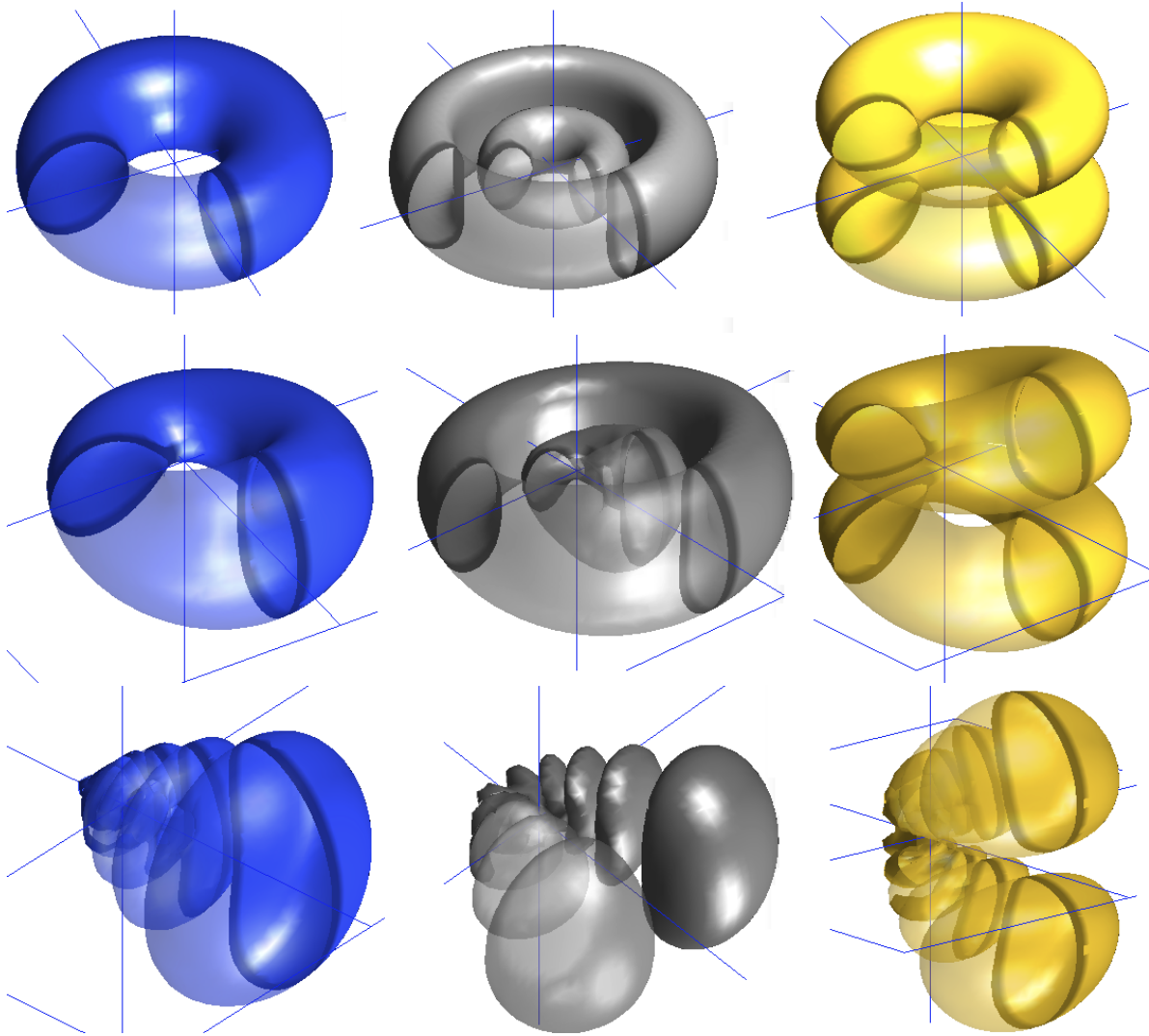


Figure 11. The coherent elliptic state (in the left column) and the two quasi-coherent elliptic states as one changes from purely circular situation, where E is zero, via elliptic region with both E and B to the Stark region where magnetic field is negligible. Note that for the quasi-coherent elliptic states the resulting Stark states are eigenstates of A_x or x but not eigenstates of L_x . This is because the two states are degenerate and thus their linear combinations can be chosen. For example, the first two states could be combined to a $m_x = 1$ and $m_x = -1$, but the connection to the "flat states" which are determined by the magnetic field dictates the indicated shapes.

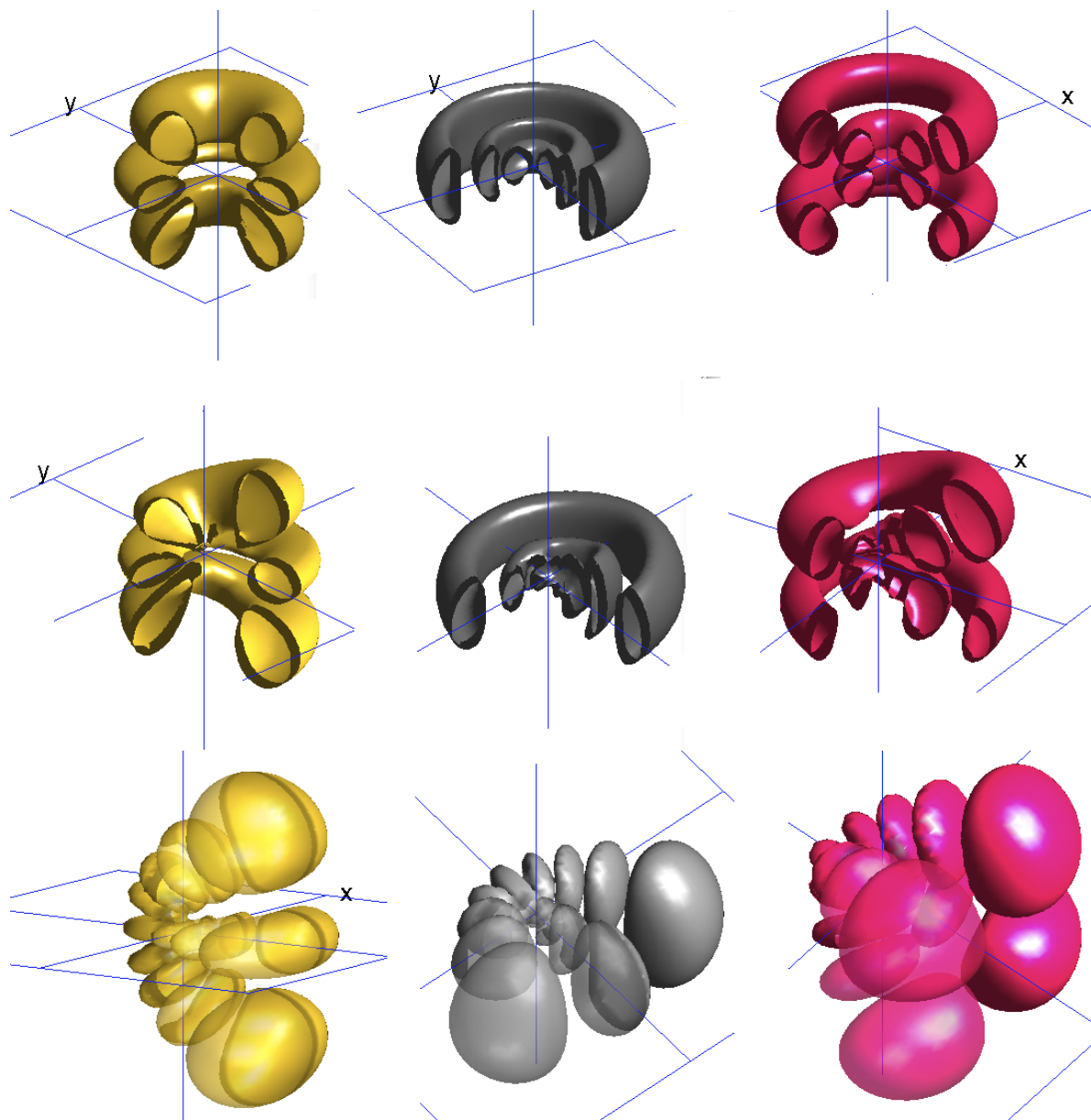


Figure 12. Three quasi-coherent elliptic states of the second type which remain degenerate as one changes from purely circular situation, where E is zero, via elliptic region with both E and B to the Stark region where magnetic field is negligible. Note that the resulting Stark states which are eigenstates of A_x or x are not necessarily eigenstates of L_x . This is because the three states are degenerate and thus their linear combinations can be chosen. The three states are $m_x = 2$ and $m_x = -2$ and $m_x = 0$, but the connection to the "flat states" which are determined by the magnetic field dictates the indicated shapes. The corresponding usually used Stark states with well defined m are shown in the figure 13 below.

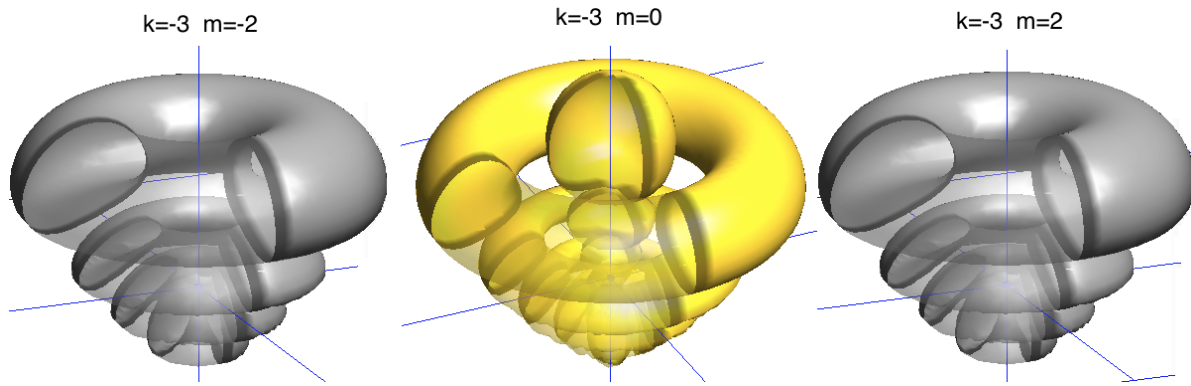


Figure 13. The three stark states which combine to the three Stark states shown in the lowest part of the figure 12. The middle one is $m = 0$, i.e. axially isotropic. Note that here the quantization axis is vertical as in the section on Stark states, while the one relevant in the previous figure is horizontal.

8. Conclusion

We have shown several types of visualizations which appear useful in understanding the shapes of various Rydberg states. In several cases found in literature the use of modifying multiplicative factors or similar procedures introduced to hide away unwanted features has led to a long propagation of partial misunderstandings. We have reviewed several such cases and show alternative visualizations.

In general, we have demonstrated that present day computer graphics can give very intuitive representations of Rydberg states.

The system used in this work is MATLAB, but very similar functionality can be found in many different frameworks, as e.g. Mathematica, Python libraries, visualization toolkit VTK and many others. The main keywords are contour plots and plots of isosurfaces for three-dimensional distributions.

An important message of this work should also be that one can not expect to be able to use the standard methods with standard parameters. Successful applications require additional research into the abilities of the software.

References

- [1] T. F. Gallagher, *Rydberg Atoms* (University Press: Cambridge) (1994)
- [2] W. Pauli, *Z. Phys.* **36**, 339 (1926), English translation in B. L. van der Waerden (Editor) *Sources of quantum mechanics* (Courier Dover Publications: New York) (1968)
- [3] Bommier A, Delande D and Gay J-C in C A Nicolaides, C W Clark and M Nayfeh (Editors) *Atoms in Strong Fields* (Plenum: New York) p 155 (1990)
- [4] C. H. Greene , A.S. Dickinson and H.R. Sadeghpour, *Phys. Rev. Lett.* **85**, 2458 (2000)
- [5] W. Li, T. Pohl, J. M. Rost, Seth T. Rittenhouse, H. R. Sadeghpour, J. Nipper, B. Butscher, J. B. Balewski, V. Bendkowsky, R. Löw and T. Pfau, *Science* **334**, 1110 (2011)
- [6] Y. N. Demkov, B. S. Monozon and V. N. Ostrovsky, *Sov. Phys. JETP*, **30**, 775 (1969)
- [7] Y. N. Demkov, V. N. Ostrovsky and E. A. Solov'ev, *Sov. Phys. JETP* **39**, 57 (1974)
- [8] A. K. Kazansky and V. N. Ostrovsky, *J. Phys. B* **29**, L855 (1996)
- [9] M. J. Engelfield, *Group Theory and the Coulomb Problem* (Wiley: New York) (1972)
- [10] M. Førre, H. M. Nilsen, and J. P. Hansen, *Phys. Rev. A*, **65**, 053409 (2002)
- [11] E. Majorana, *Nuovo Cimento* **9**, 43 (1932)
- [12] L. D. Landau and E. M. Lifschits, *Quantum Mechanics* (Pergamon Press: Oxford) (1976)
- [13] J. Pollet, O. Méplan, and C. Gignoux, *Phys. A: Math. Gen.* **28**, 7287 (1995)
- [14] J. C. Gay, D. Delande and A. Bommier, *Phys. Rev. A*, **39**, 6587 (1989)
- [15] K B MacAdam and E Horsdal-Pedersen, *J. Phys. B* **36**, R167 (2003)
- [16] J. C. Day, T. Ehrenreich, S. B. Hansen, E. Horsdal-Pedersen, K. S. Mogensen, and K. Taulbjerg, *Phys. Rev. Lett.* **72**, 1612 (1994).
- [17] K. S. Mogensen, J. C. Day, T. Ehrenreich, E. H. Pedersen, and K. Taulbjerg, *Phys. Rev. A* **51**, 4038 (1995).
- [18] L. Kocbach, *Physica Scripta* **T46**, 261 (1993)